Electronic Supplementary Material (ESI) for Dalton Transactions.

Supporting information

For

Photocatalytic reactivity tuning by heterometal and addenda metal variation in Lindqvist polyoxometalates

Johannes Tucher[a,b], Stefanie Schlicht[b], Fabian Kollhoff[b] and Carsten Streb*[a,b]

[a]Institute of Inorganic Chemistry I, Ulm University, Albert-Einstein-Allee 11, 89081 Ulm, Germany. carsten.streb@uni-ulm.de

[b]Department Chemistry and Pharmacy, Friedrich-Alexander-University Erlangen-Nuremberg, Egerlandstr. 1, 91058 Erlangen, Germany.

1. Instrumentation

NMR spectroscopy: ^{1}H- and ^{13}C-NMR spectroscopy was performed on a JEOL EX 270 NMR spectrometer or JEOL EX 400 spectrometer using deuterated solvents as internal standards.

UV-Vis spectroscopy: UV-Vis spectroscopy was performed on a Shimadzu UV-2401PC spectrophotometer or Varian Cary 50 spectrophotometer. All systems were used with standard cuvettes (d = 10.0 mm).

FT-IR spectroscopy: FT-IR spectroscopy was performed on a Shimadzu FT-IR-8400S spectrometer. Samples were prepared as KBr pellets. Signals are given as wavenumbers in cm^{-1} using the following abbreviations: vs = very strong, s = strong, m = medium, w = weak and b = broad.

Elemental analysis: Elemental analysis was performed on a Euro Vector Euro EA 3000 Elemental Analyzer.

Flame atomic absorption spectroscopy: Flame atomic absorption spectroscopy (FAAS) was performed on a Perkin Elmer 5100 PC Atomic Absorption System.

Electrospray ionization mass spectrometry: ESI-MS spectra were recorded on a Bruker Daltonics maXis ultra high resolution ESI-Time-Of-Flight MS. Spectra were obtained in negative-ion mode. Peaks were identified using simulated isotopic patterns created within the Bruker DataAnalysis software.

General remarks: All chemicals were purchased from Sigma Aldrich, ABCR or ACROS and were of reagent grade. The chemicals were used without further purification unless stated otherwise. $(^{n}Bu_4N)_2[Mo_6O_{19}]$[S1] $(^{n}Bu_4N)_4[\alpha\text{-}Mo_8O_{26}]$,[S1] and $(^{n}Bu_4N)_4[V_4O_{12}]$[S2] were prepared according to literature references.

2. Synthetic section:

Synthesis of compound 1: $(^{n}Bu_4N)_3[VMo_5O_{19}]$:

Synthesis of compound **1** is a modification of the original synthesis reported by Klemperer *et al*:[S1] $(^{n}Bu_4N)_4[\alpha\text{-}Mo_8O_{26}]$ (0.242 g, 112 μmol) and $(^{n}Bu_4N)_4[V_4O_{12}]$ (0.677 g, 496 μmol) are suspended in a N,N-dimethylformamide-water mixture (10 ml, 20:1, v:v). After heating to 80°C, the solid materials dissolved and the solution colour intensified to a deep yellow. At this point, 70 mg (1.3 mmol) ammonium chloride are added and the solution is kept at 80°C for 2 h after which the colour had changed to light yellow and slight precipitation was observed. After centrifugation, the yellow solution was crystallized by diffusion of ethyl acetate, giving orange crystals of single-crystal XRD quality as the only solid product. The crystals were washed with diethyl ether and dried under vacuum. Yield: 90 mg, (57 μmol, 32 % based on Mo).

Elemental analysis for $C_{48}H_{108}N_3VMo_5O_{19}$ (Mw: 1562.02 g/mol) in wt.-% (calcd.): C 37.09 (36.91), H 7.15 (6.97), N 2.84 (2.69), V 2.62 (3.24), Mo 31.91 (31.16).

Characteristic IR bands (in cm^{-1}): 2959 (m), 2874 (s), 1481 (vs), 1152 (m), 976 (s), 935 (s), 874 (s), 795 (s).

Characteristic UV-Vis signals (in acetonitrile): $\lambda_{max,1}$ = 219 nm, ε= 1.70 x 10^4 M^{-1} cm^{-1}; $\lambda_{max,2}$ = 265 nm, ε= 1.41 x 10^4 M^{-1} cm^{-1}; $\lambda_{max,3}$ = 332 nm, ε= 0.66 x 10^4 M^{-1} cm^{-1}; $\lambda_{max,4}$ = 425 nm, ε= 1.12 x 10^3 M^{-1} cm^{-1} (shoulder).

Synthesis of compound 2: $(^{n}Bu_4N)_3[VW_5O_{19}]$:

Synthesis of compound **2** is a modification of the original synthesis reported by Klemperer *et al*:[S3] $Na_2WO_4 \cdot 2\ H_2O$ (9.07 g, 27.5 mmol) and V_2O_5 (0.5 g, 2.75 mmol) were dissolved in H_2O (30 ml) by adding aqueous NaOH (6 M) dropwise and heating the reaction mixture to 80°C. The resulted, clear solution was adjusted to pH 2.8 with HCl (6 M). After one hour heating the yellow solution was cooled to room temperature and precipitated by adding $^{n}Bu_4NBr$ (5.87 g, 18.2 mmol). The lemon yellow product was

filtered off and washed several times with H_2O (50 ml) and dried in the desiccator. Yield: 2.66 g (1.33 mmol, 24.2 % based on W).

Elemental analysis for $C_{48}H_{108}N_3VW_5O_{19}$ (Mw: 2001.52 g/mol) in wt.-% (calcd.): C 29.07 (28.80), H 5.52 (5.44), N 2.12 (2.10), V 2.04 (2.55), W 45.31 (45.93).

Characteristic IR bands (in cm^{-1}): 2960 (vs), 2872 (s), 1482 (vs), 1382 (m), 1152 (w), 952 (vs), 886 (m), 801 (vs).

Characteristic UV-Vis signals (in acetonitrile): $\lambda_{max,1}$ = 217 nm, ε= 1.63 x 10^4 M^{-1} cm^{-1}; $\lambda_{max,2}$ = 265 nm, ε= 1.16 x 10^4 M^{-1} cm^{-1}; $\lambda_{max,3}$ = 391 nm, ε= 2.43 x 10^3 M^{-1} cm^{-1}.

Synthesis of compound 3: (^{n}Bu$_4$N)$_3$Na[V$_2$Mo$_4$O$_{19}$]:

$Na_2MoO_4 \cdot 2\ H_2O$ (7.84 g, 32.4 mmol) and V_2O_5 (1.0 g, 5.50 mmol) were dissolved in H_2O (20 ml) by adding aqueous NaOH (6 M) dropwise and heating the reaction mixture to 80°C. The resulting solution was adjusted to pH 5.0 with HCl_{aq} (6 M). After two hours, the pale orange solution was cooled to room temperature and precipitated by adding ^{n}Bu$_4$NBr (3.06 g, 9.49 mmol). The pale orange product was filtered off and washed several times with H_2O (50 ml) and dried in the desiccator. Yield: 4.60 g (2.99 mmol, 36.9 % based on Mo).

Elemental analysis for $C_{48}H_{108}N_3NaV_2Mo_4O_{19}$ (Mw: 1540.01 g/mol) in wt.-% (calcd.): C 37.04 (37.44), H 7.03 (7.07), N 2.70 (2.73), V 6.42 (6.62), Mo 24.79 (24.92), Na 1.38 (1.49).

Characteristic IR bands (in cm^{-1}): 2960 (vs), 2872 (s), 1482 (vs), 1383 (m), 1152 (m), 978 (m), 933 (vs), 884 (m), 791 (vs).

Characteristic UV-Vis signals (in acetonitrile): $\lambda_{max,1}$ = 224 nm, ε= 4.35 x 10^4 M^{-1} cm^{-1}; $\lambda_{max,2}$ = 258 nm, ε= 2.73 x 10^4 M^{-1} cm^{-1}; $\lambda_{max,3}$ = 318 nm, ε= 1.20 x 10^4 M^{-1} cm^{-1}.

Synthesis of compound 4: (^{n}Bu$_4$N)$_3$Na[V$_2$W$_4$O$_{19}$]:

$Na_2WO_4 \cdot 2\ H_2O$ (6.46 g, 19.58 mmol) and V_2O_5 (1.0 g, 5.50 mmol) were dissolved in H_2O (20 ml) by adding aqueous NaOH (6 M) dropwise and heating the reaction mixture to 80°C. The resulting solution was adjusted to pH 5.0 with HCl_{aq} (6 M). After one hour, the orange solution was cooled to room temperature and precipitated by adding ^{n}Bu$_4$NBr (6.0 g, 18.6 mmol). The orange product was filtered off and washed several times with H_2O (50 ml) and dried in the desiccator. Yield: 2.9 g (1.53 mmol, 31.3 % based on W).

Elemental analysis for $C_{48}H_{108}N_3NaV_2W_4O_{19}$ (Mw: 1891.61 g/mol) in wt.-% (calcd.): C 30.04 (30.48), H 5.73 (5.75), N 2.18 (2.22), V 5.29 (5.39), W 38.79 (38.87), Na 1.12 (1.22).

Characteristic IR bands (in cm^{-1}): 2960 (vs), 2873 (s), 1482 (vs), 1383 (m), 1152 (w), 974 (m), 950 (vs), 886 (m), 804 (vs), 740 (m).

Characteristic UV-Vis signals (in acetonitrile): $\lambda_{max,1}$ = 209 nm, ε= 2.55 x 10^4 M^{-1} cm^{-1}; $\lambda_{max,2}$ = 233 nm, ε= 1.58 x 10^4 M^{-1} cm^{-1} (shoulder); $\lambda_{max,3}$ = 366 nm, ε= 1.28 x 10^4 M^{-1} cm^{-1} (plateau).

3. Electrospray ionization mass spectrometry (ESI-MS)

ESI-mass spectrometry for {VMo_5}

ESI-MS measurements were performed on (^{n}$Bu_4N)_3[VMo_5O_{19}]$ ([{VMo_5} *ca*. 5 x 10^{-5} M in acetonitrile) in negative (-ve) ion mode. Data analysis showed that the base peaks and several other high-intensity peaks were associated with the $[VMo_5O_{19}]^{3-}$ ion. No other cluster ions (e.g. $[V_xMo_{6-x}O_{19}]^{n-}$; x ≠ 1) were observed. Detailed peak assignments are given in Table S2, see Figure S2 below.

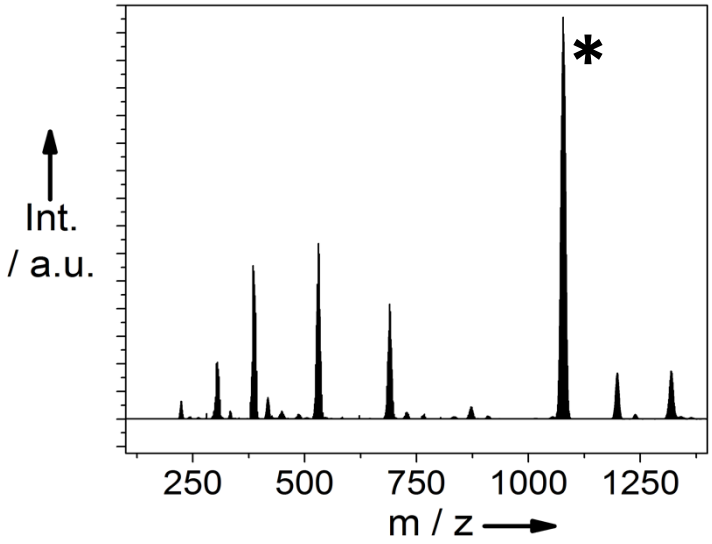

Figure S1: Negative-mode ESI-mass spectrum for a solution of **1**, (^{n}$Bu_4N)_3[VMo_5O_{19}]$ in acetonitrile ([**1**] *ca.* 5 x 10^{-5} M). The main product (∗) at m/z = 1077.66 corresponds to {(^{n}Bu_4N)$H[VMo_5O_{19}]$}$^-$, for further details see Table S2.

Table S2: Negative mode ESI-MS assignments for **1**:

m/z	calculated m/z	Assigned species	Charge
223.82	223.84	$\{Mo_3O_{10}\}^{2-}$	2-
304.68	304.69	$\{HMo_2O_7\}^{-}$	1-
386.69	386.72	$\{VMo_2O_9\}^{-}$	1-
417.67	417.70	$\{H_1VMo_5O_{19}\}^{-}$	1-
530.62	530.61	$\{VMo_3O_{12}\}^{-}$	1-
1077.66	1077.68	$\{(^nBu_4N)H[VMo_5O_{19}]\}^{-}$	1-
1198.81	1198.82	$\{(^nBu_4N)_3H[VMo_5O_{19}]_2\}^{2-}$	2-
1318.95	1318.96	$\{(^nBu_4N)_2[VMo_5O_{19}]\}^{-}$	1-

ESI-mass spectrometry for $\{VW_5\}$

ESI-MS measurements were performed on $(^nBu_4N)_3[VW_5O_{19}]$ ([$\{VW_5\}$ *ca*. 5 x 10^{-5} M in acetonitrile) in negative (-ve) ion mode. Data analysis showed that the base peaks and several other high-intensity peaks were associated with the $[VW_5O_{19}]^{3-}$ ion. No other cluster ions (e.g. $[V_xW_{6-x}O_{19}]^{n-}$; $x \neq 1$) were observed. Detailed peak assignments are given in Table S3, see Figure S3 below.

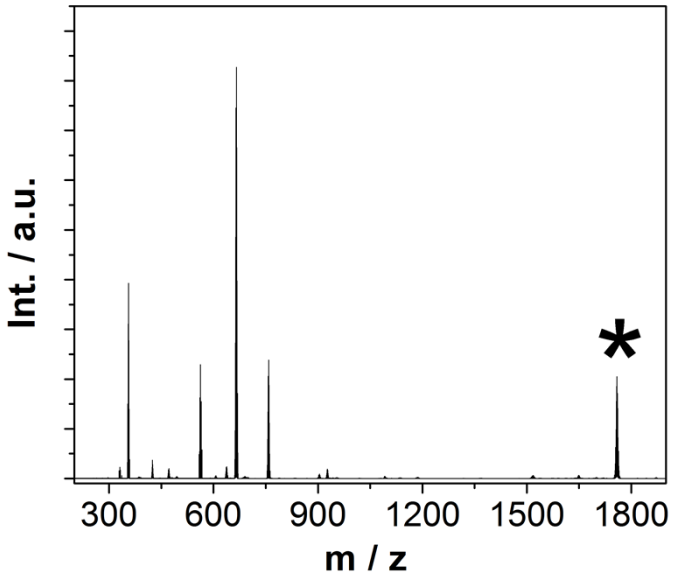

Figure S2: Negative-mode ESI-mass spectrum for a solution of **2**, $(^{n}Bu_4N)_3[VW_5O_{19}]$ in acetonitrile ([**2**] *ca.* 5 x 10^{-5} M). The main product **(∗)** at m/z = 1759.16 corresponds to $\{(^{n}Bu_4N)_2[VW_5O_{19}]\}^-$, for further details see Table S3.

Table S3: Negative mode ESI-MS assignments for **2**:

m/z	calculated m/z	Assigned species	Charge
355.87	355.90	$\{W_3O_{10}\}^{2-}$	2-
562.77	562.80	$\{VW_2O_9\}^-$	1-
665.81	665.80	$\{Na(H_2O)_2[VW_5O_{19}]\}^{2-}$	2-
758.44	758.44	$\{(^{n}Bu_4N)VW_5O_{19}\}^{2-}$	2-
1759.15	1759.16	$\{(^{n}Bu_4N)_2VW_5O_{19}\}^-$	1-

ESI-mass spectrometry for $\{V_2Mo_4\}$

ESI-MS measurements were performed on $(^{n}Bu_4N)_3Na[V_2Mo_4O_{19}]$ ([$\{V_2Mo_4\}$ *ca*. 5 x 10^{-5} M in acetonitrile) in negative (-ve) ion mode. Data analysis showed that the base peaks and several other high-intensity peaks were associated with the $[V_2Mo_4O_{19}]^{4-}$ ion. No other cluster ions (e.g. $[V_xMo_{6-x}O_{19}]^{n-}$; $x \neq 1$) were observed. Detailed peak assignments are given in Table S4, see Figure S4 below.

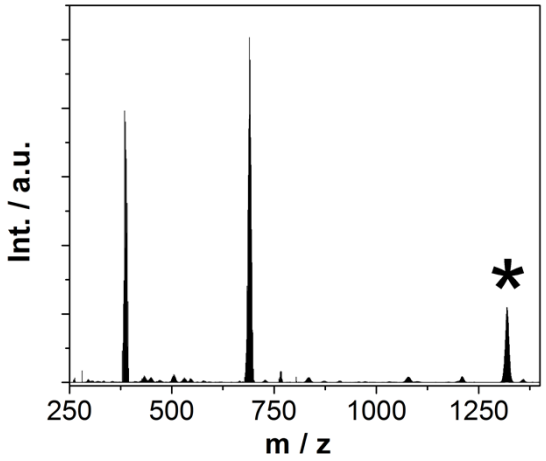

Figure S3: Negative-mode ESI-mass spectrum for a solution of **3**, $(^{n}Bu_4N)_3Na[V_2Mo_4O_{19}]$ in acetonitrile ([**3**] *ca.* 5 x 10^{-5} M). The main product (∗) at m/z = 1319.91 corresponds to $\{(^{n}Bu_4N)_2H(MeCN)_5Na(H_2O)_6[V_2Mo_4O_{19}]\}^-$ for further details see Table S4.

Table S4: Negative mode ESI-MS assignments for **3**:

m/z	calculated m/z	Assigned species	Charge

384.69	384.71	$\{V_1Mo_2O_9\}^-$	1-
689.97	689.95	$\{(^nBu_4N)Mo_3O_{10}\}^-$	1-
1319.91	1319.89	$\{(^nBu_4N)_2H(MeCN)_5Na(H_2O)_6[V_2Mo_4O_{19}]\}^-$	1-

ESI-mass spectrometry for $\{V_2W_4\}$

ESI-MS measurements were performed on $(^nBu_4N)_3Na[V_2W_4O_{19}]$ ([$\{V_2W_4\}$ *ca*. 5 x 10^{-5} M in acetonitrile) in negative (-ve) ion mode. Data analysis showed that the base peaks and several other high-intensity peaks were associated with the $[V_2W_4O_{19}]^{4-}$ ion. No other cluster ions (e.g. $[V_xW_{6-x}O_{19}]^{n-}$; $x \neq 1$) were observed. Detailed peak assignments are given in Table S5, see Figure S5 below.

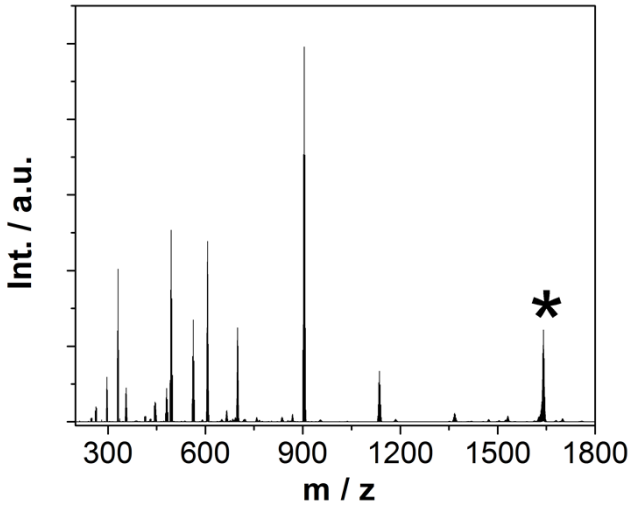

Figure S4: Negative-mode ESI-mass spectrum for a solution of **4**, $(^nBu_4N)_3Na[V_2W_4O_{19}]$ in acetonitrile ([**4**] *ca.* 5 x 10^{-5} M). The main product (∗) at m/z = 1641.14 corresponds to $\{(^nBu_4N)_1H_2(CH_3OH)_3(CH_3CN)_3(H_2O)_3[V_2W_4O_{19}]\}^-$, for further details see Table S5.

Table S5: Negative mode ESI-MS assignments:

m/z	calculated m/z	Assigned species	Charge
330.85	330.87	$\{VWO_6\}^-$	1-
494.88	494.89	$\{(MeO)W_2O_6\}^-$	1-
562.79	562.80	$\{VW_2O_9\}^-$	1-
606.84	606.84	$\{(NH_4)_2(H_2O)_2V_2W_4O_{19}\}^{2-}$	2-
699.42	699.43	$\{(C_4H_{12}N)_2(CH_3CN)(CH_3OH)(H_2O)_2V_2W_4O_{19}\}^{2-}$	2-
1641.09	1641.07	$\{(^nBu_4N)H_2(CH_3OH)_3(CH_3CN)_3(H_2O)_2V_2W_4O_{19}\}^-$	1-

4. UV-Vis spectroscopic investigations

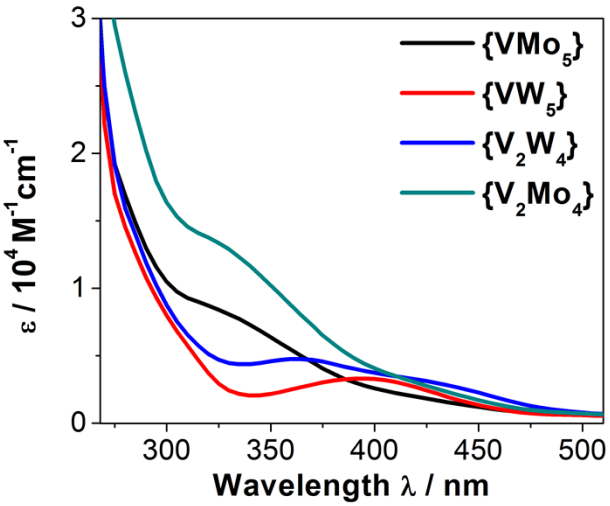

Figure S5: UV-Vis spectroscopic analysis of **1** - **4** in N, N-dimethyl formamide, showing the tailing of the LMCT transitions into the visible region.

5. Photooxidation reactions

The following mechanism is reported in the literature for the hydroxyl radical mediated substrate photooxidation by polyoxometalate clusters (see references 1e, 3, 32, main manuscript).

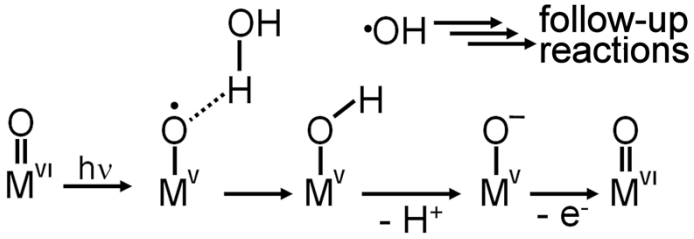

Figure S6: Hydroxyl radical-mediated substrate photooxidation by polyoxometalate clusters. Irradiation of a O→M ligand to metal charge-transfer band leads to a charge-separated state and formation of an oxo-centered radical on the cluster shell. Reaction of the oxo radical with pre-associated water leads to hydrogen-atom abstraction and

hydroxyl radical formation. The hydroxyl radical dissociates from the cluster shell and undergoes follow-up oxidative reactions.

Photooxidations were performed by dissolving **1** - **4** and indigo in N,N-dimethyl formamide (DMF). Clear, homogeneous solutions were obtained. The solutions were irradiated using LED light sources in custom-built irradiation setups. Standard light source was a LED with λ_{max} = 430 nm, $P_{nominal}$ = 3 W. Standard molar ratios were $[Ind]_0$: $[1]_0$ – $[4]_0$ = 5 : 1. Deaerated experiments were performed by de-gassing the samples with Argon for 10 min prior to the experiment. As blank references, identical samples as described above without added photocatalyst **1** - **4** were used.

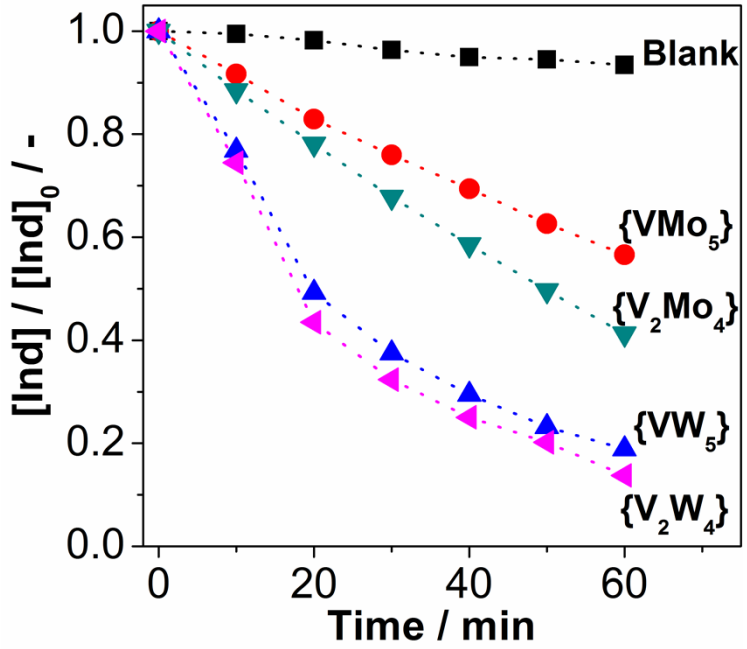

Figure S7: Photocatalytic aerated Ind decomposition catalyzed by **1** - **4**. Conditions: LED-irradiation, λ_{max} = 430 nm, $P_{nominal}$ = 3 W; N,N-dimethyl formamide (aerated). $[Ind]_0$ = 5.0 µM; $[\mathbf{1}]_0$ – $[\mathbf{4}]_0$ = 1.0 µM. Ind = Indigo.

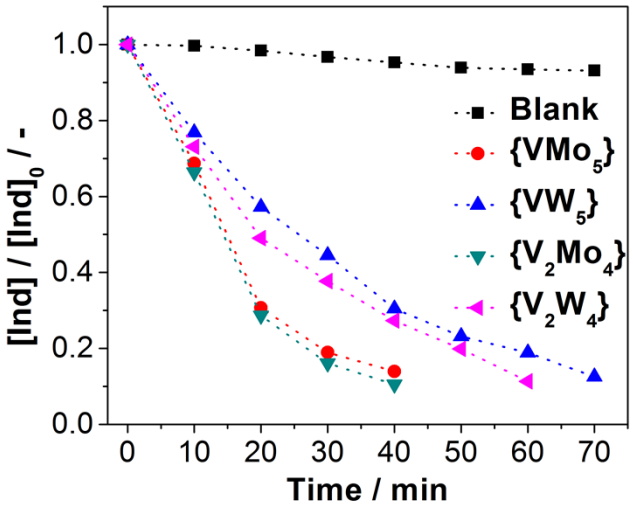

Figure S8: Photocatalytic de-aerated Ind decomposition catalyzed by **1** - **4**. Conditions: LED-irradiation, λ_{max} = 430 nm, $P_{nominal}$ = 3 W; N,N-dimethyl formamide; the de-aerated samples were de-gassed with Ar for 10 min prior to the experiment. $[Ind]_0$ = 5.0 µM; $[\mathbf{1}]_0$ – $[\mathbf{4}]_0$ = 1.0 µM. Ind = Indigo.

6. Quantum efficiency determination

Quantum efficiencies were determined using a custom-built irradiation and quantum efficiency determination setup reported by König, Riedle *et al*., see reference 18, main manuscript.

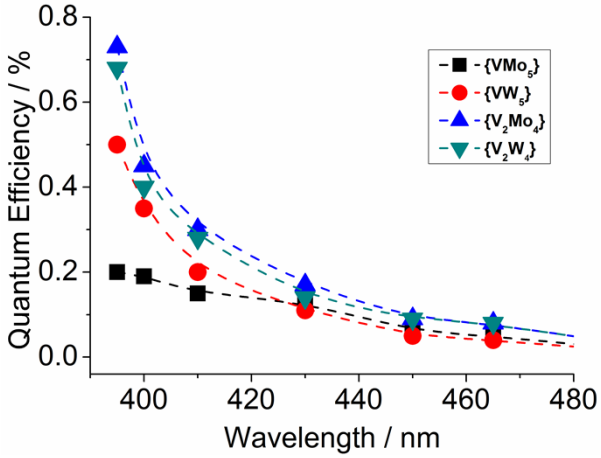

Figure S9: Quantum efficiencies for the Ind photooxidation by **1** to **4** as a function of wavelength. Conditions: solvent: DMF, [Ind]:[cluster] = 1:1; $[Ind]_0$ = 1.0 µM, $[cluster]_0$ = 1.0 µM. Ind = Indigo.

Table S6: Quantum efficiency determination for the indigo photooxidation by **1 - 4**

λ / nm	{VMo_5} / QE / %	{VW_5} / QE / %	{V_2Mo_4} / QE / %	{V_2W_4} / QE / %
395	0.2	0.5	0.73	0.68
400	0.19	0.35	0.45	0.4
410	0.15	0.2	0.3	0.28
430	0.13	0.11	0.17	0.14
450	0.11	0.05	0.09	0.09
465	0.1	0.04	0.08	0.08
505	0	0	0	0

7. Hydroxyl scavenging experiments

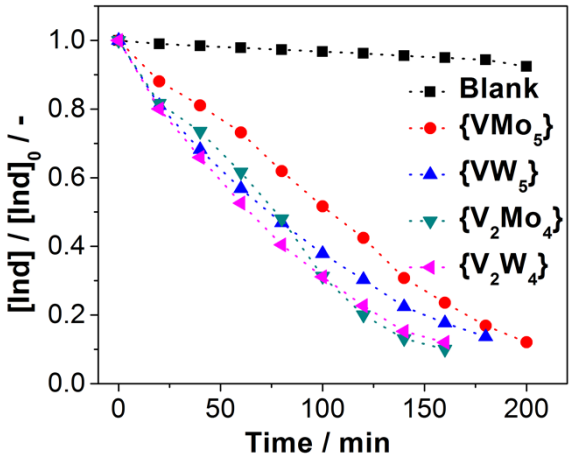

Figure S10: Photocatalytic indigo decomposition catalyzed by **1** - **4** in the presence of ethanol (EtOH) under aerated conditions. Conditions: LED-irradiation, λ_{max} = 430 nm, $P_{nominal}$ = 3 W; solvent: N,N-dimethyl formamide (DMF, aerated). $[Ind]_0$ = 5.0 µM; $[\mathbf{1}]_0$ – $[\mathbf{4}]_0$ = 1.0 µM, $[EtOH]_0$ = 50 µM. Ind = Indigo.

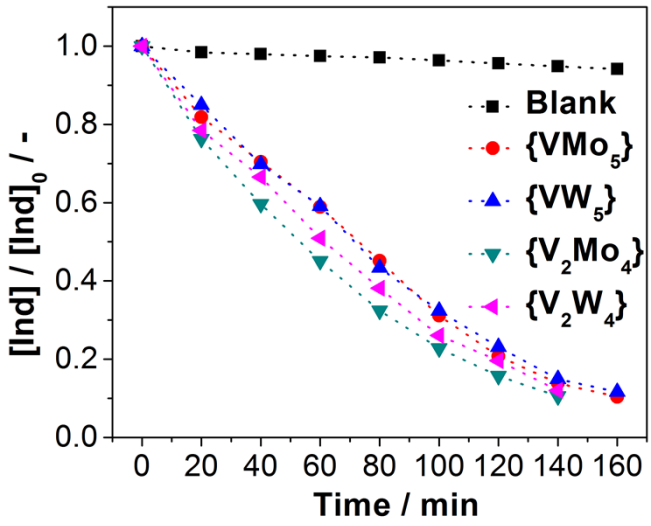

Figure S11: Photocatalytic indigo decomposition catalyzed by **1** - **4** in the presence of ethanol (EtOH) under de-aerated conditions. Conditions: LED-irradiation, λ_{max} = 430 nm, $P_{nominal}$ = 3 W; solvent: N,N-dimethyl formamide (DMF, de-aerated). $[Ind]_0$ = 5.0 µM; $[\mathbf{1}]_0$ – $[\mathbf{4}]_0$ = 1.0 µM, $[EtOH]_0$ = 50 µM. Ind = Indigo.

8. Recyclability of 1 to 4

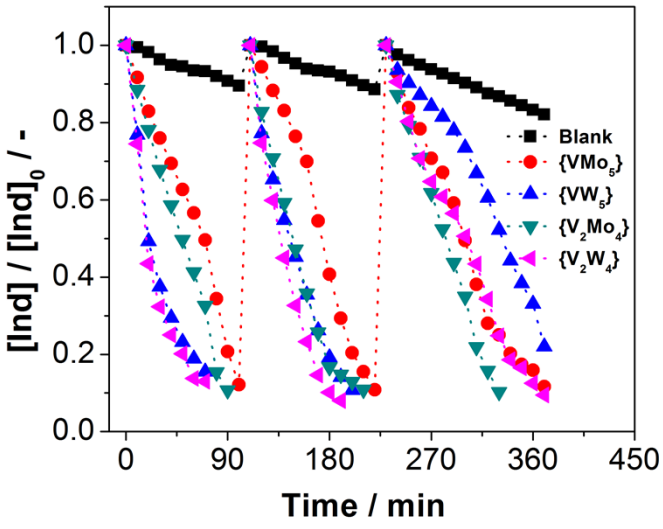

Figure S12: Recyclability of **1** - **4** as homogeneous indigo photooxidation catalysts under aerated conditions. Run 1 to Run 3 were performed at $[Ind]_0$: $[\mathbf{1}]_0$ – $[\mathbf{4}]_0$ = 5 : 1. Conditions: solvent: DMF (aerated), light source: monochromatic LED (λ_{max} = 430 nm, $P_{nominal}$ = 3 W).

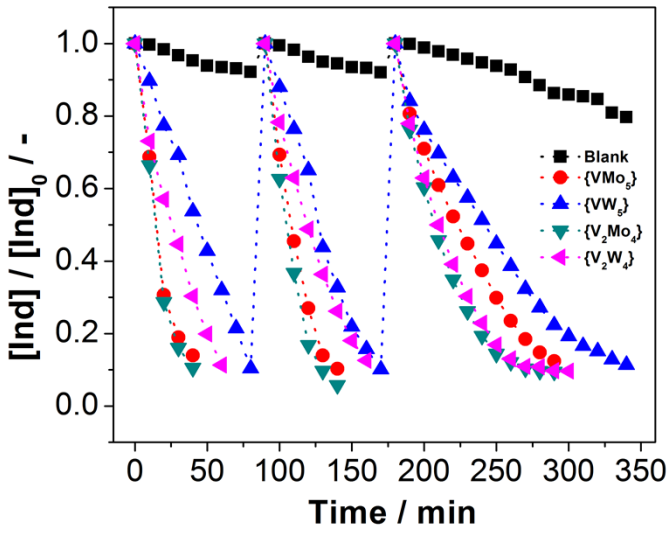

Figure S13: Recyclability of **1** - **4** as homogeneous indigo photooxidation catalysts under de-aerated conditions. Run 1 to Run 3 were performed at $[Ind]_0$: $[\mathbf{1}]_0$ – $[\mathbf{4}]_0$ = 5 : 1. Conditions: solvent: DMF (de-aerated), light source: monochromatic LED (λ_{max} = 430 nm, $P_{nominal}$ = 3 W).

9. Literature references cited in Supporting Information

[S1] M. Filowitz, R. K. C. Ho, W. G. Klemperer, W. Shum, *Inorg. Chem.* **1979**, *18*, 93-103.

[S2] J. Forster, B. Rösner, M. M. Khusniyarov, C. Streb, *Chem. Commun.* **2011**, *47*, 3114.

[S3] M. Filowitz, R. K. C. Ho, W. G. Klemperer, W. Shum, *Inorg. Chem.* **1979**, *18*, 93-103.